

A Procedure for Estimation of Source and Propagation Amplitude Corrections for Regional Seismic Discriminants

Steven R. Taylor
Hans E. Hartse

Earth and Environmental Sciences Division
Geophysics Group, EES-3
Los Alamos National Laboratory
Los Alamos, NM 87545

May 30, 1997

LAUR-97-2017

Submitted to *J. Geophys. Res.*

Abstract

We outline a procedure for the estimation of frequency-dependent source and propagation amplitude corrections for regional seismic discriminants (Source Path Amplitude Correction - SPAC). For a given station and phase, a number of well-recorded earthquakes are inverted for source and path corrections. The method assumes a simple Brune (1970) earthquake-source model and a simple propagation model consisting of a frequency-independent geometrical spreading and frequency-dependent power-law Q . The inverted low-frequency levels are then regressed against m_b to derive a set of corrections that are a function of m_b and distance. Once a set of corrections are derived, effects of source scaling and distance as a function of frequency are applied to amplitudes from new events *prior* to forming discrimination ratios. The resulting discriminants are normally distributed and amenable to multivariate feature selection, classification, and outlier techniques. To date, most discrimination studies have removed distance corrections once a particular amplitude ratio is formed (Distance Corrected Ratio - DCR). DCR generally works well for phase ratios taken in a particular frequency band. However, when different frequency bands are combined (for phase spectral ratios or cross spectral ratios), significant source-scaling effects (e.g. corner-frequency scaling) can remain, causing the discriminants to vary as a function of event size and to be non-normally distributed. It is then often necessary to construct non-physical transformations in an attempt to make the discriminants multivariate normal. The SPAC technique can be used to construct discriminants that are multivariate normal by using simple physical seismic source and propagation models. Moreover, phase amplitude residuals as a function of frequency can be spatially averaged and used as additional path-specific corrections to correct for additional propagation effects such as phase blockages.

Introduction

Numerous types of regional seismic discriminants have been proposed to aid in the identification of clandestine nuclear explosions (e.g. Pomeroy *et al.*, 1983; Taylor *et al.*, 1989; Walter *et al.*, 1995). The discriminants can be grouped into three principal classes: 1) P to S phase ratios (e.g. $\log(P_g / L_g)$ or $m_b - M_s$), 2) phase spectral ratios (e.g. $\log[P_g(0.75 - 1.5 \text{ Hz}) / P_g(4 - 8 \text{ Hz})]$), and 3) P to S cross-spectral ratios which basically combine 1 and 2 above (e.g. $\log[P_g(4-8 \text{ Hz}) / L_g(1-2 \text{ Hz})]$). These discriminants can show significant regional variability and performance. One difficult problem associated with constructing discriminants is related to the various corrections that are applied to them. To date, research has focused mainly on deriving propagation (e.g. distance) corrections. However, for discriminants that involve measurements in different frequency bands (classes 2 and 3 above), source scaling can be a significant factor causing trends with source size (e.g. Taylor and Denny, 1991). If multivariate techniques are to be used for feature selection and event classification, it is important that biases caused by both propagation *and* source effects be removed. In this paper, we outline a procedure for simultaneously correcting for both propagation and source effects prior to forming discriminants.

A number of approaches for removing propagation effects have been utilized that are generally effective to a certain degree. One promising approach is to use observable parameters representing waveguide effects between a given source and station (such as topography and/or basin thickness) to correct discriminants (e.g. Zhang *et al.*, 1994). Another, more commonly used approach that we term Distance Corrected Ratios (DCR) is illustrated in Figure 1 for the P_g spectral ratio in the 0.75 to 1.5 Hz and 4 to 8 Hz bands recorded at the Chinese Digital Seismic Station, WMQ (for details see Hartse *et al.*, 1997). In Figure 1, a subset of P_g earthquake spectral ratios having good signal to noise are regressed versus the logarithm of the distance. The coefficients from the linear regression are then applied to both the earthquake and nuclear explosion populations resulting in distance-corrected spectral ratios. For the case shown in Figure 1, it can be seen that application of the distance correction significantly improves the separation of the earthquake and explosion populations.

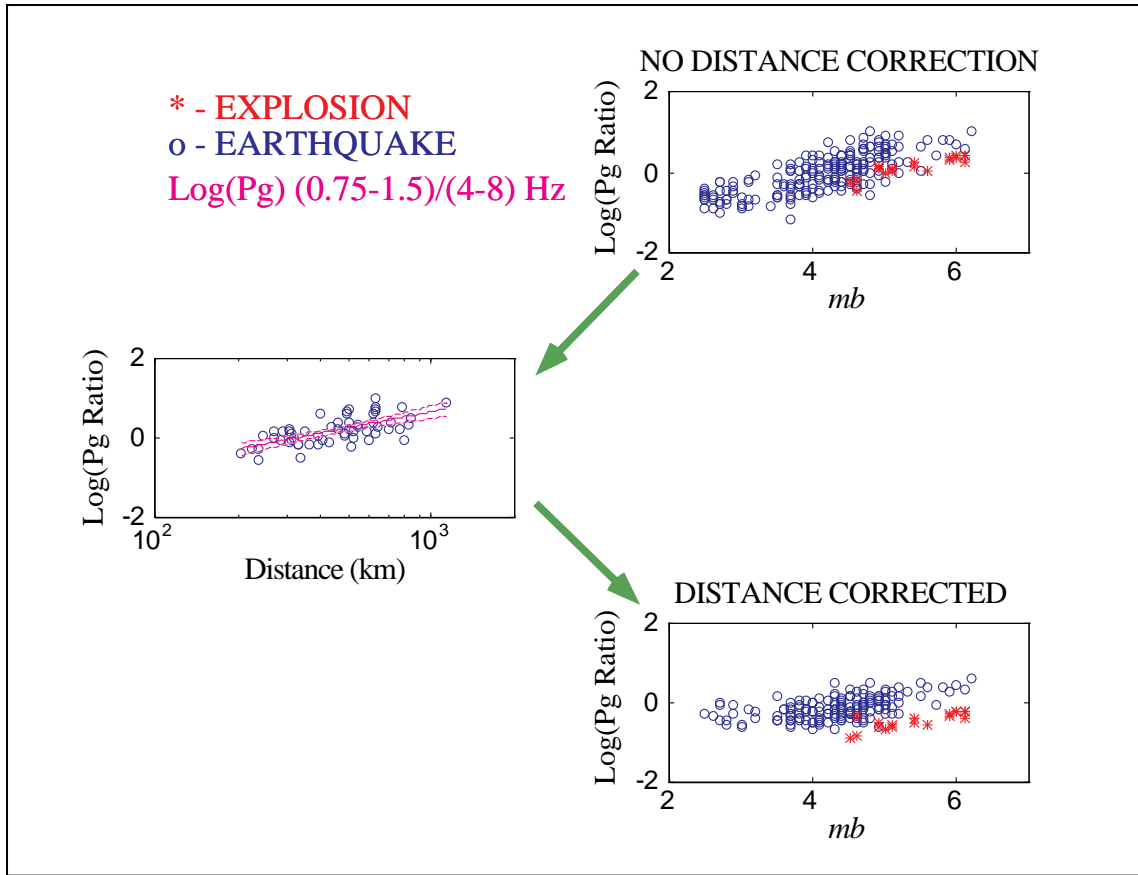


Figure 1. Illustration of the Distance Corrected Ratio (DCR) technique commonly used for applying distance corrections to a P_g spectral ratio discriminant. Upper right panel shows uncorrected spectral ratios for earthquakes and nuclear explosions at WMQ (Hartse *et al.*, 1997). Left panel shows earthquake P_g spectral ratios for events with a signal-to-noise ratio greater than 10 regressed versus the logarithm of the distance. Lower right panel shows distance-corrected P_g spectral ratio. Notice dependence of the spectral ratio with magnitude remains.

However, there are a number of drawbacks to the DCR approach. First, in regions having complicated geophysical structure, the distance corrections can vary significantly depending on the subset chosen for regression. Second, development of the distance corrections can be cumbersome if many discriminants are being investigated. Third, and possibly most importantly, is that application of the distance correction does not remove effects caused by source scaling. This is illustrated in the lower right panel of Figure 1 where it can be seen that the P_g spectral ratio is flat at small magnitudes and then gradually increases for m_b greater than about 4. This effect is generally observed with any discriminant that combines measurements in different frequency bands and is partly a

consequence of source corner frequency scaling (*e.g.* Taylor and Denny, 1991). Because the corner-frequency scaling remains, the discriminants will not be normally distributed and not amenable to analysis by most multivariate discrimination methods. It is then necessary to construct non-physical transformations (such as Box-Cox transformations; *e.g.* Hand (1981)) in an attempt to make the discriminants multivariate normal. The SPAC technique we describe below can be used to construct discriminants that are multivariate normal by using simple physical models for the seismic source and propagation.

In this paper, we discuss a new approach to the derivation and application of corrections for both source and propagation effects which we term the Source Path Amplitude Correction (SPAC) technique. A set of frequency-dependent corrections can be developed for a particular station to correct each phase for attenuation and source scaling *prior* to forming a discriminant. Additionally, after first-order corrections are derived for a given station, the amplitude residuals can be spatially averaged in some sense and used to further correct for propagation effects (such as phase blockages) from specific source regions.

After the corrections are made, we will show that multivariate-normal discriminants can be directly constructed that have reduced scatter and improved separation between earthquake and explosion populations. Because the discriminants are multivariate normal, they can be used in multivariate feature selection studies and in event classification schemes (*e.g.* Hand, 1981) or outlier detection approaches (Fisk *et al.*, 1996; Taylor and Hartse, 1997).

Inversion for Source and Path Parameters

In this section we describe the method we use for inverting for source and path parameters and forming a set of frequency-dependent amplitude corrections for each phase recorded at a given station. In theory, the results could be extended to handle data from a network of stations. In our formulation, we basically follow the technique of Sereno *et al.*, (1988) with minor modifications.

At a particular station, we assume the instrument-corrected amplitude spectrum for a given phase, $A_i(f)$, for source i , is given by

$$A_i(f) = \frac{S_i(f)}{r^\eta} \exp\left(-\frac{\pi f}{Q(f)v} r\right) \quad (1)$$

where $S_i(f)$ is the source spectrum, r is the epicentral distance (km), η is the frequency-independent geometrical spreading coefficient, f is the frequency, $Q^{-1}(f)$ is the frequency-dependent attenuation, and v is the group velocity. We linearize equation (1) by taking logarithms

$$\log A_i(f) + \eta \log r_i = \log S_i(f) - \frac{\pi f \log e}{Q(f)v} r_i \quad (2)$$

In equation (2) we assume a simple Brune (1970) dislocation source model

$$S_i(f) = \frac{S_0^{(i)}}{1 + \left(\frac{f}{f_c^{(i)}}\right)^2} \quad (3)$$

where for event i , $S_0^{(i)}$ is the low-frequency spectral level and $f_c^{(i)}$ is the source corner frequency. In equation (3), we explicitly assume a high-frequency decay of -2 which is commonly observed for earthquakes (e.g. Hough, 1996).

We assume a power-law frequency-dependent Q of the form

$$Q(f) = Q_0 f^\gamma \quad (4)$$

We further assume a simple scaling between event corner frequency and low frequency spectral level of the form

$$f_c = c S_0^{-\kappa} \quad (5)$$

For a Brune (1970) dislocation source model, $\kappa = 1/3$ and c is proportional to the cube root of the Brune stress drop, σ_b . Although some studies have argued for an increase of stress drop with moment, in general there has been no definitive scaling observed (e.g. Hough, 1996). Additionally, the scaling of corner-frequency and moment (or low-frequency level) has been observed to deviate from 1/3. For example, Cong *et al.*, (1996) and Nuttli (1983) have observed $\kappa = 1/4$ from central Asian earthquakes and mid-plate earthquakes, respectively.

Inserting equations (3), (4), and (5) into (2) gives the final equation to be inverted

$$\log A_i(f) + \eta \log r_i = \log S_o^{(i)} - \log \left[1 + \left(\frac{f(S_o^{(i)})^\kappa}{c} \right)^2 \right] - \frac{\pi \log e}{Q_0 \nu} f^{1-\gamma} r_i \quad (6)$$

In practice, we solve for a low-frequency level for each event, $S_o^{(i)}$, and for γ . We set η , Q_0 , and κ and search on c . Equation (6) is nonlinear and we perform an iterative linearized inversion by computing the first-order partial derivatives using a Gauss-Newton method.

As discussed by Sereno *et al.*, (1988) there exist many tradeoffs in the different parameters for inverting an equation of the form of (6). Our philosophy in deriving source and path corrections is to constrain as many parameters as possible based on prior information. The remaining parameters are checked to see if they are geophysically reasonable. The key is treating the problem as a nonunique curve-fitting exercise to derive reasonable corrections to be applied to seismic amplitudes used as discriminants.

Inversion Results

The data used in this study are described in detail in Hartse *et al.*, (1997). We have chosen P_g and L_g data recorded at the Chinese Digital Seismic Station WMQ. All seismograms were obtained from the IRIS Data Management Center. The data are from 27 nuclear explosions (1 from Lop Nor and 26 from the east Kazakh test site), and 525 earthquakes (152 from PDE catalogs and 373 from the State Seismological Bureau (SSB) Chinese catalogs; Gao and Richards, 1994). Distances range from 200 to 1200 km and magnitudes from 2.5 to 6.1. Event locations and magnitudes were obtained from both the United States Geological Survey Preliminary Determination of Epicenters (USGS/PDE) catalogs maintained at the Incorporated Research Institutions in Seismology Data Management Center (IRIS DMC) and the Chinese State Seismological Bureau (SSB) for 1988-1989. We measured RMS amplitudes taken in 8 different 1 octave frequency bands ranging from 0.5 to 12 Hz. Because the methodology discussed above is for a spectral inversion, we convert the RMS amplitudes to pseudo-spectral amplitudes using Parseval's Theorem for the discrete Fourier transform (Oppenheim and Schaffer, 1975) which in our case involves multiplying the RMS amplitude by the phase window length. To obtain pseudo spectral displacement values, the seismograms can be corrected to displacement and RMS values computed directly. Alternatively, RMS values from seismograms corrected to ground velocity can be divided by 2π times the frequency of the filter (which is the

approach we have taken). As discussed by Rodgers *et al.*, (1997), the RMS amplitudes can be biased high relative to log averaged frequency-domain amplitudes. To mitigate this effect, we assign the low frequency cutoff to be the specified frequency for each band.

For both P_g and L_g we selected a subset of earthquakes for inversion having all 8 frequency measurements passing a signal-to-noise (using pre- P_n noise) of 10. This resulted in 22 and 68 earthquakes for the P_g and L_g inversions, respectively. It should be noted that we performed inversions including earthquakes having at least 6 or 7 frequency measurements with little change in the final results. Because we have converted to pseudo spectra, we use a geometrical spreading factor of $\eta = 1/2$ for L_g . Geometrical spreading factors for P_g are much less certain. Using reflectivity synthetics, Campillo *et al.*, (1984) inferred time-domain geometrical spreading rates (η) of 0.83 for L_g (close to the Airy phase theoretical value of $5/6$, [Nuttli, 1973]) and 1.5 for P_g . Because the time-domain spreading rate for P_g is approximately a factor of 2 greater than L_g , we chose $\eta = 1$ for frequency-domain P_g . The propagation of P_g and other regional phases are strongly controlled by crustal structure and assumptions of geometrical spreading rates are subject to much uncertainty. As discussed by Sereno *et al.*, (1988), the choice of geometrical spreading trades off with the values of the low-frequency level, S_0 , which does not affect our final results.

The value of Q_0 for L_g was set to be 400 based on previous work around WMQ of Cong *et al.*, (1996). Based on observational results in the western U.S., Paul *et al.*, (1996) found similar values of Q_0 for P_g and L_g so we set the Q_0 value for P_g to be 400. Again, the choice Q_0 of will affect the mean of the low-frequency levels and not the frequency-dependence of the attenuation which does not affect our final results.

The results of the inversion for P_g and L_g are listed in Table 1 and shown in Figures 2 and 3, respectively.

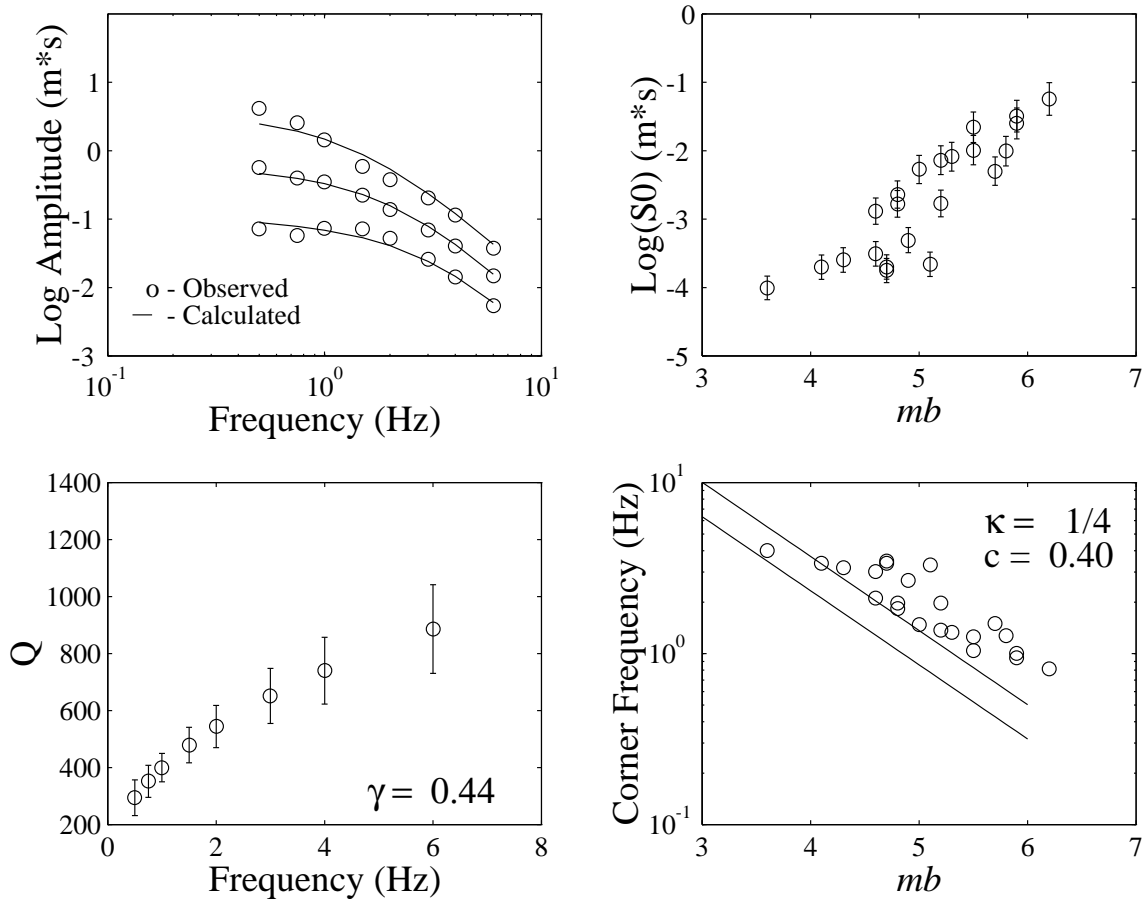


Figure 2. Results from inversion of earthquake P_g pseudo spectrum using equation (6). Geometrical spreading factor (η) assumed to be 1. Upper left; calculated and observed spectra for 3 randomly chosen events. Lower left; frequency-dependent Q values, 95% confidence limits, and γ (Q_0 set to 400). Upper right; logarithm of the low-frequency level, S_0 , versus m_b and 95% confidence limits. Lower right, corner frequency (estimated from equation 5) versus m_b . Also shown are theoretical curves for S -wave corner frequency using a Brune (1970) dislocation source model (where $\kappa = 1/3$) for stress drops of 5 and 20 MPa (50 and 200 bars; lower and upper curves, respectively)

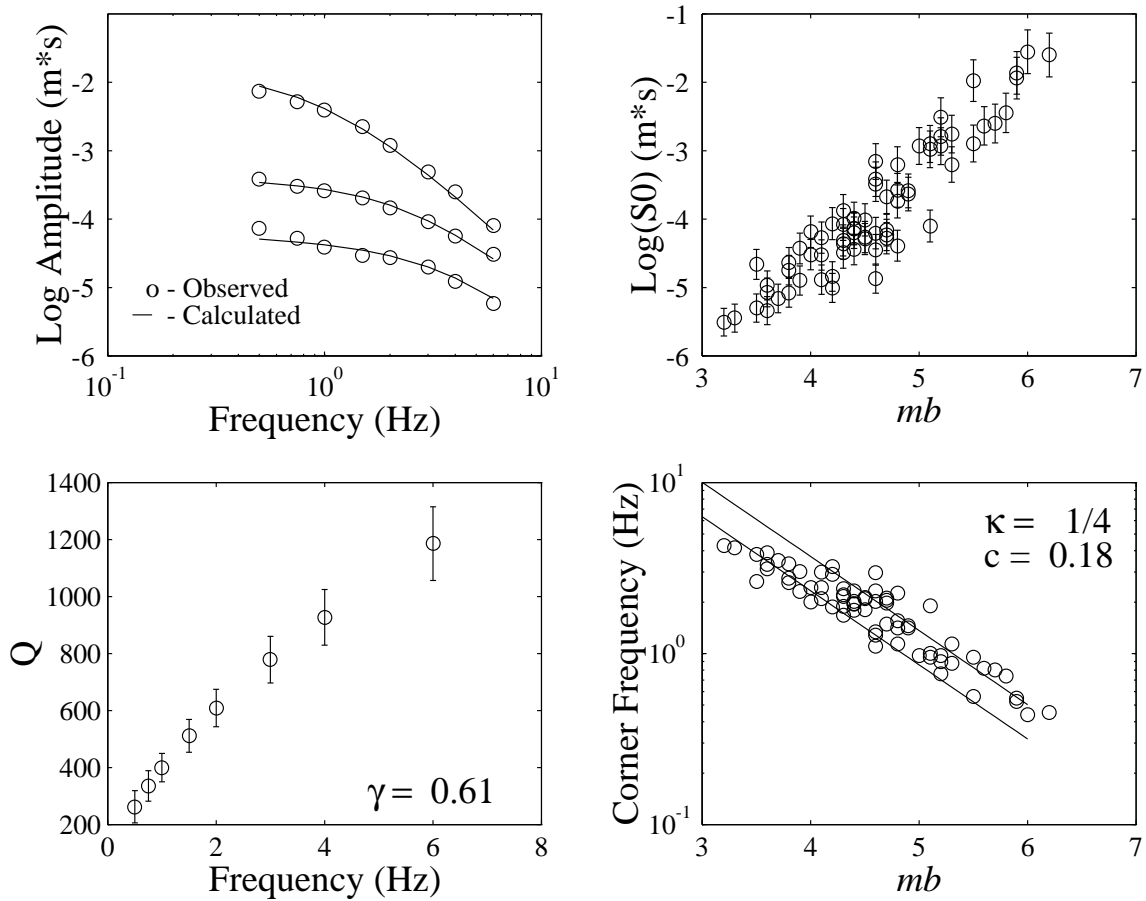


Figure 3. Same as Figure 2, except for L_g .

Table 1
Inversion Results for P_g and L_g (MKS)

Phase	κ	η	Q_0	ν	c	γ	$\hat{\sigma}_d$	$\log S_0$
P_g	1/4	1	400	6100	0.40	0.44+/-0.06	0.11	$1.2m_b - 8.6$
L_g	1/4	1/2	400	3500	0.18	0.61+/-0.06	0.13	$1.4m_b - 10.4$
L_g	1/3	1/2	400	3500	0.07	0.71+/-0.05	0.15	$2.0m_b - 12.9$

For L_g , runs were made with κ set to 1/4 and 1/3 (Table 1). In general, the runs having $\kappa = 1/4$ gave a scaling of the low-frequency level with magnitude (and moment) closer to that expected by theory and from previous studies, more reasonable corner frequencies and γ values. The scaling of $\log S_0$ with m_b for linear regressions are listed in Table 1. The fits to the data were generally quite good as illustrated in the upper left

portion of Figures 2 and 3. Thus, in this study, we will use the results for the inversions having $\kappa = 1/4$. For these runs, the corner frequencies are also consistent with those expected from the Brune (1970) dislocation source model for reasonable stress drops (using $f_c = 0.49V_s(\sigma_b/M_0)^{1/3}$). For the 22 events in common, $f_c(P_g)/f_c(L_g) = 1.6$ which is very close to the P to S corner-frequency shift commonly reported in the literature (e.g. Hanks, 1981).

Application of Source and Path Amplitude Corrections (SPAC)

Once the parameters are obtained for equation (6), the amplitudes from other events can be corrected for source scaling and propagation using SPAC. To do this, it is first necessary to obtain an estimate of the low-frequency level, S_0 . We have chosen to tie the low-frequency level to magnitude through the linear relation $\log S_0 = am_b + b$. Seismic moment would work as well, however, only a very small subset of earthquakes used in this study had published moments. As will be seen below, a problem with the tie to m_b is caused by uncertainties in the SSB magnitudes and their relationship to PDE magnitudes. We are uncertain as to how the magnitudes in the SSB catalogs were calculated. We suspect that the SSB magnitudes may be from a coda magnitude scale (e.g. Bakun *et al.*, 1985). In actual monitoring situations, it is assumed that more reliable regional magnitude scales will be available. Additionally, the relationship between magnitude and moment (or low-frequency level) can be complicated by source scaling and may not be linear over a broad range of magnitudes (e.g. Nuttli, 1983). To illustrate the technique, we will use magnitudes from both the SSB and PDE catalogs and show that the overall effect on seismic discriminants is small. The results from the regression for the three runs are given in Table 1.

For a new event of unknown source type but known location, we select recorded RMS amplitudes having signal-to-noise ratios greater than 2. The available amplitudes are converted to pseudo-spectral displacement as discussed previously. The low-frequency level is estimated from the m_b value using the regression coefficients given in Table 1. Equation (6) is then used to derive a predicted phase amplitude and the logarithm of the corrected amplitude, $A_i^{(c)}(f)$, is defined to be the difference between the logarithm of the observed, $A_i^{(o)}(f)$, and predicted, $A_i^{(p)}(f)$, pseudo-spectral values. Explicitly

$$\log A_i^{(c)}(f) = \log A_i^{(o)}(f) - \log A_i^{(p)}(f) \quad (7)$$

where the observed pseudo-spectral amplitude is given by

$$\log A_i^{(o)}(f) = \log A_i(f) + \eta \log r_i \quad (8)$$

and the predicted pseudo-spectral amplitude is

$$\log A_i^{(p)}(f) = \log S_o^{(i)} - \log \left[1 + \left(\frac{f(S_o^{(i)})^\kappa}{c} \right)^2 \right] - \frac{\pi \log e}{Q_0 \nu} f^{1-\gamma} r_i \quad (9)$$

where the low-frequency level is set from the magnitude using the coefficients for a and b from the relation, $\log S_0 = am_b + b$ and other parameters given in Table 1. Note that the corrected amplitudes given in equation (7) are basically residuals to the fit given by equation (6) where S_o has been tied to m_b . In this way, an event having large phase amplitudes at a particular frequency will be characterized by a large positive residual.

The results of applying the correction for the $\kappa = 1/4 L_g$ run (Table 1) are shown in Figure 4 for 273 earthquakes having signal-to-noise ratios greater than 2 in the frequency band 0.75 to 1.5 Hz. The top portion of the figure shows uncorrected RMS amplitudes versus m_b and distance. The uncorrected data spans approximately 4 orders of magnitude. The bottom portion of Figure 4 shows the corrected amplitudes (pseudo spectrum) versus m_b and distance. After corrections are applied, the data span approximately 2 orders of magnitude and trends with distance and magnitude are largely eliminated. There appears to be an increase of corrected amplitude with decreasing m_b below about magnitude 4. The effect is most pronounced for earthquakes having m_b values obtained from the SSB catalogs. It appears that this effect is due to the fact that the SSB magnitudes are biased low relative to the PDE magnitudes below magnitude 4. In this case, the predicted amplitudes will be smaller and the corrected amplitudes (observed - predicted amplitudes) will be larger as observed in Figure 4. This observation highlights the need for accurately estimated magnitudes in a CTBT monitoring environment.

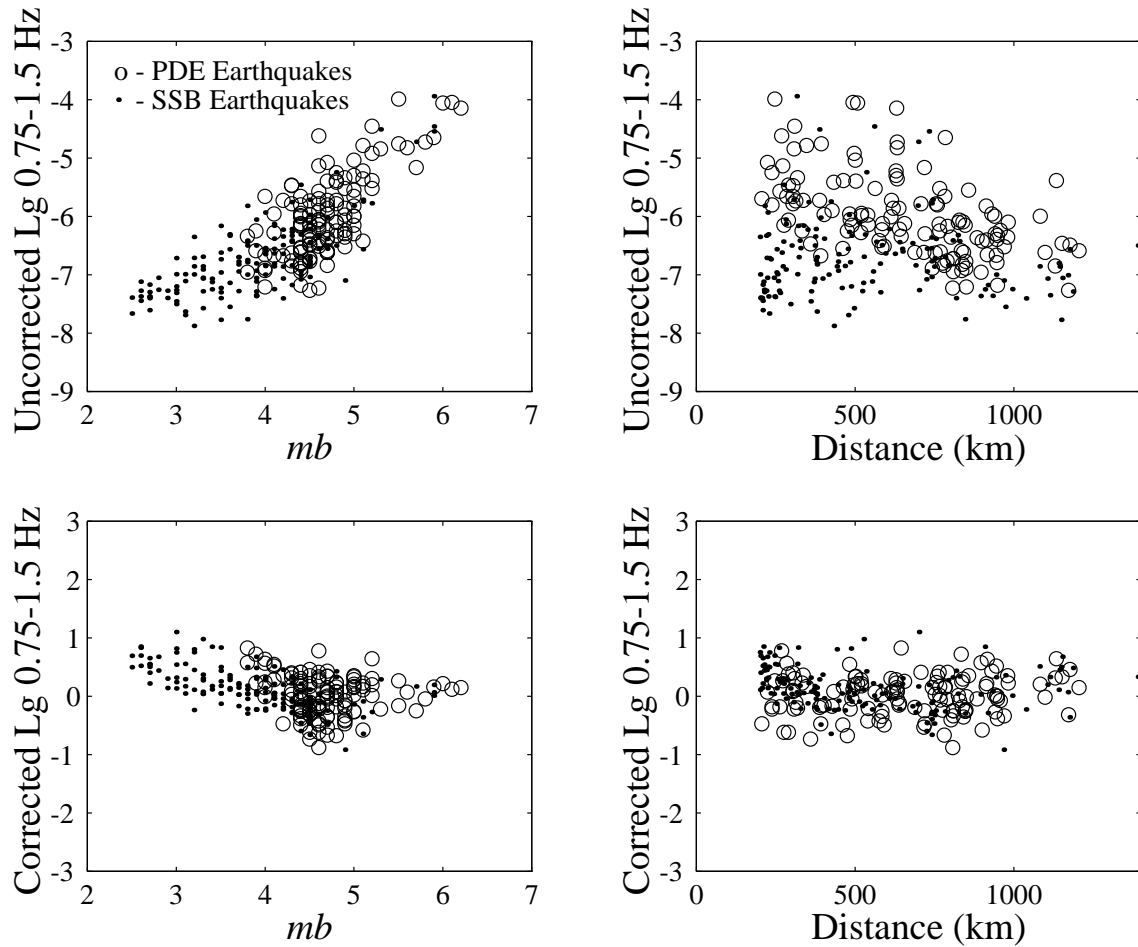


Figure 4. Uncorrected (top) and corrected using SPAC (bottom) L_g amplitudes in the 0.75 to 1.5 Hz frequency band versus m_b (left) and distance (right) for 273 earthquakes having signal-to-noise values greater than 2. Earthquakes from the PDE and SSB catalogs are shown as open circles and dots, respectively.

We also corrected the P_g amplitudes using Equation (6) and the parameters listed in Table 1 and then formed the P_g spectral ratio of the 0.75 to 1.5 and 4 to 8 Hz bands (Figure 5). The top portion of Figure 5 compares the P_g spectral ratio versus m_b for the distance correction derived from the spectral ratio (as illustrated in Figure 1) and for the combined source and path correction for both earthquakes and nuclear explosions. Although the dislocation source model used in correcting the amplitudes is not appropriate for nuclear explosions, we still use it because in an actual monitoring situation, the source type would be unknown. Also note that the magnitude problems noted in Figure 4, do not seriously affect the final P_g spectral ratio in Figure 5.

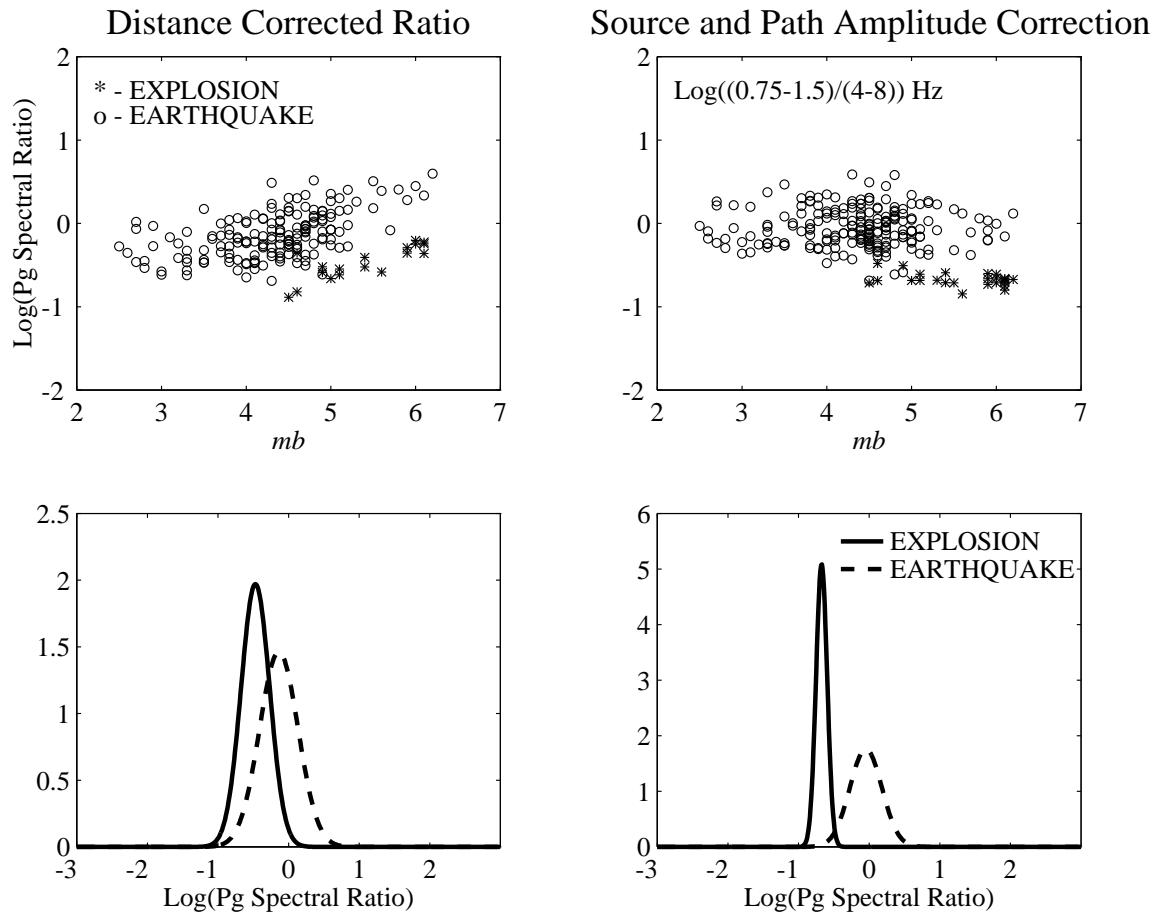


Figure 5. Comparison of DCR (left) and SPAC (right) techniques. P_g spectral ratio of the 0.75 to 1.5 and 4 to 8 Hz bands versus m_b using the distance correction method illustrated in Figure 1 (top left) and using the combined source and path corrections listed in Table 1 (upper right) for earthquakes and nuclear explosions described in Hartse *et al.*, (1997). Normal probability density function for P_g spectral ratio of earthquakes and nuclear explosions using just distance correction (lower left) and combined source and path corrections (lower right).

As described above, for the upper left portion of Figure 5, the P_g spectral ratio was formed for earthquakes having good signal-to-noise ratio and then regressed versus the logarithm of distance. The distance correction factors were then applied to all P_g spectral ratios for earthquakes and nuclear explosions having signal-to-noise values greater than 2 (Figure 1). The corner frequency scaling still is evident in this case as an increase in the spectral ratio with magnitude. The overlap between the two populations is illustrated in the lower left portion of the figure using the estimated normal probability density function.

Visually, the P_g ratio with just the distance correction plotted versus m_b appears to show good separation between earthquakes and explosions. However, m_b is never actually used as a discrimination variable and a multivariate discrimination method would see the projection of the spectral ratio on the ordinate. For the SPAC method, the trend with m_b is removed and the separation and variance projected on the ordinate are improved and reduced, respectively (compare Figure 5 lower left with lower right). Table 2 lists the earthquake and explosion mean and standard deviations and a measure of the one-dimensional Mahalanobis distance between the earthquake and explosion populations, D^2 (Hand, 1981) given by

$$D^2 = \frac{(\bar{R}_x - \bar{R}_Q)^2}{\sigma_x^2 + \sigma_Q^2} \quad (10)$$

where \bar{R}_x and \bar{R}_Q are the mean spectral ratios for the explosions and earthquakes, respectively. σ_x^2 and σ_Q^2 are the variance for the explosions and earthquakes, respectively. Multivariate estimates of the Mahalanobis distance are often used in discrimination and feature selection procedures (e.g. Taylor, 1996).

Table 2
Comparison of Corrected P_g Spectral Ratio

	\bar{R}_x	σ_x	\bar{R}_Q	σ_Q	D^2
DCR	-0.47	0.20	-0.14	0.27	0.95
SPAC	-0.67	0.08	-0.05	0.23	6.80

\bar{R}_x - mean spectral ratio for explosions

σ_x - standard deviation for explosions

D^2 Mahalanobis distance (equation 7)

The combined source and path corrections (SPAC) result in a value of D^2 that is a factor of 7 greater than that from applying the distance correction to the spectral ratios (DCR). This is because the difference in the mean spectral ratio for the earthquakes and explosions increases and the variance for each decreases for the combined source and path correction.

Using the P_g spectral ratios in Figure 5, we performed a goodness of fit hypothesis test to determine whether the data follow a Gaussian distribution (e.g. Menke, 1984). For

the DCR and SPAC, the χ^2 values were 19.0 and 17.8, respectively. At the 5% level of significance, we rejected the null hypothesis, H_0 , that the P_g spectral ratios are normally distributed for DCR, but accepted H_0 for SPAC.

An area of future research is motivated by the maps shown in Figure 6. The L_g residuals from equation (7) in the 0.75 to 1 Hz band have been plotted on a map. The left portion of the figure shows that, in general, larger amplitudes are observed to the south and east of WMQ. Smaller amplitudes are observed to the west and southwest along the Tien Shan. The shaded map in the right portion of Figure 6 shows results by averaging the residuals in 1 degree bins.

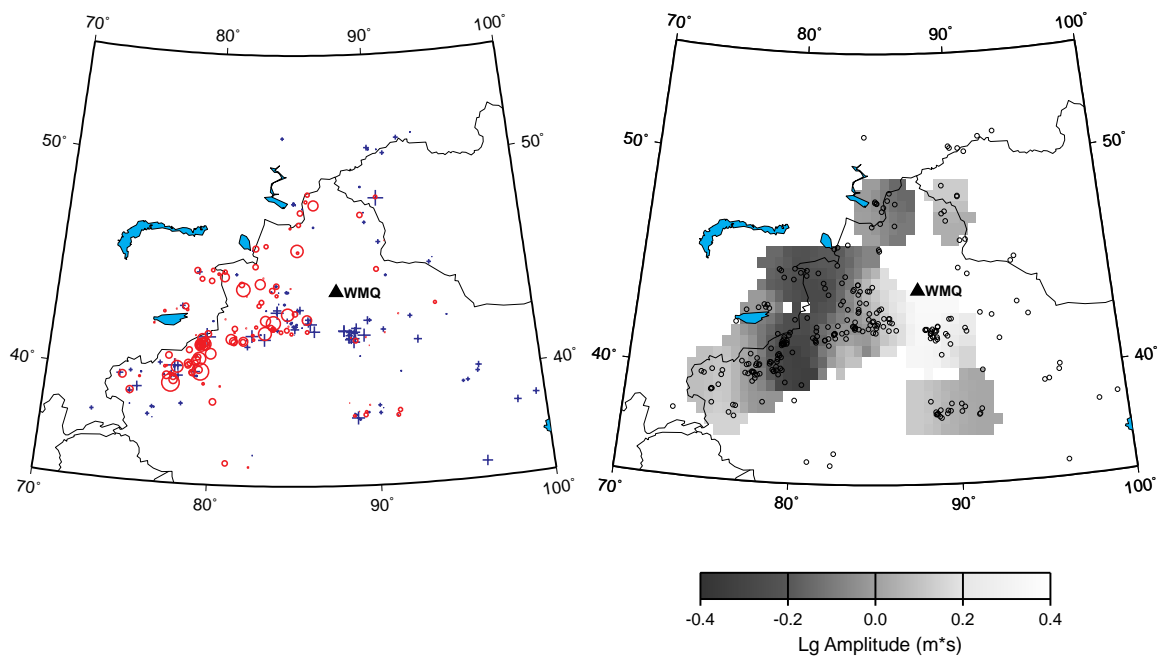


Figure 6. L_g amplitude residuals in the 0.75 to 1.5 Hz band for earthquakes (equation 7). Left: individual residuals where + indicates positive residual (large amplitude) and o indicates negative residual (small amplitude). Size of symbol corresponds to size of residual. Right: Shaded map where residuals in left portion of figure have been spatially averaged in 1 degree bins having a minimum of 5 residuals. Shading scale given on bottom where darker shades indicate negative residuals and lighter shades positive residuals.

Once a large dataset has been processed and inverted for a particular station, the residuals can be spatially averaged into bins of specified sizes depending on the data distribution. These can then be used as additional amplitude corrections that account for effects along specific source/receiver paths. For example, in the amplitude inversion

(equation 6), if a phase is attenuated or blocked between the station and a particular source region, then that region will be characterized by large negative corrections. These corrections can be applied to those of equation (7) further reducing the scatter in the discriminant. It will be necessary to treat these corrections with some caution because they may be affected by factors such as source depth and focal mechanism. But, as shown by Phillips (1997), they may serve as an empirical alternative to techniques proposed by Zhang *et al.*, (1994) that depend on knowledge of specific path parameters.

Conclusions

We have described a technique (Source and Path Amplitude Corrections - SPAC) for simultaneously correcting regional seismic discriminants for source scaling and path effects at a particular station. Because the SPAC method is based on simple source and propagation models, it requires few assumptions and is reasonably simple to implement. In practice, once a station is established and a catalog of regional earthquakes is acquired, seismic amplitudes in different frequency bands can be measured and inverted for the source and path corrections. Because of the nonuniqueness inherent with the inversion, some subjectivity is involved in deciding which model to use. We have found, however, that some range of parameter flexibility can be used without seriously affecting the final results. One strength of the SPAC method is that the absolute amplitudes for each phase are corrected as a function of frequency. Once this is done, distance- and source-corrected discriminants can be formed directly from the corrected amplitudes. The resulting discriminants are normally distributed and amenable to analysis by most feature selection, classification, and outlier detection techniques. The parameters used to correct the amplitudes can easily be updated as more data are acquired.

Acknowledgments

Helpful discussions with Howard Patton, W. Scott Phillips, and George Randall are appreciated. We also appreciate reviews of the manuscript by W. Scott Phillips and Howard Patton. This work is performed under the auspices of the U.S. Department of Energy by Los Alamos National Laboratory under contract W-7405-ENG-36.

References

- Anderson, T.W., Introduction to Multivariate Statistical Analysis, Wiley, New York, 675pp, 1984.
- Bakun, W.H., L. Yizheng, F.G. Fischer, and J. Yafu, Magnitude and seismic moment scales in western Yunnan, Peoples Republic of China, *Bull. Seism. Soc. Am.*, 75, 1599-1612, 1985.
- Brune, J.N., Tectonic stress and spectra of seismic shear waves from earthquakes, *J. Geophys. Res.*, 75, 4997-5009, 1970.
- Campillo, M., M. Bouchon, and B. Massinon, Theoretical study of the excitation, spectral characteristics, and geometrical attenuation of regional seismic phases, *Bull. Seis. Soc. Am.*, 74, 79-90, 1984.
- Cong, L., J. Xie, and B.J. Mitchell, Excitation and propagation of L_g from earthquakes in central Asia with implications for explosion/earthquake discrimination, *J. Geophys. Res.*, 101, 27,779-27,789, 1996.
- Fisk, M.D., H.L. Gray, and G.D. McCartor, Regional event discrimination without transporting thresholds, *Bull. Seis. Soc. Am.*, 86, 1545-1558, 1996.
- Gao, L. and P.G. Richards, Studies of earthquakes on and near Lop Nor, China, nuclear test site, *Proceedings of the 16th Annual DARPA/AF Seismic Research Symposium*, 106-112, 1994.
- Hand, D.J., *Discrimination and Classification*, Wiley, New York, 218pp, 1981.
- Hanks, T.C., The corner frequency shift, earthquake source models, and Q, *Bull. Seis. Soc. Am.*, 71, 597-612, 1981.
- Hartse, H.E., S.R. Taylor, W.S. Phillips, and G.E. Randall, Regional event discrimination in central Asia with emphasis on western China, *Los Alamos National Laboratory, Los Alamos, NM*, LAUR-96-2002, 45 pp, submitted to *Bull. Seism. Soc. Am.*, 1996.
- Haykin, S., *Neural Networks*, Macmillan College Publishing Co., Inc., Englewood Cliffs, NJ, 695pp., 1993.
- Hough, S.E., Observational constraints on earthquake source scaling: understanding the limits in resolution, *Tectonophys.*, 261, 83-95, 1996.
- Menke, W., *Geophysical Data Analysis: Discrete Inverse Theory*, Academic Press, New York, 260pp, 1984.
- Nuttli, O.W., Seismic wave attenuation and magnitude relations for eastern North America, *J. Geophys. Res.*, 78, 876-885, 1973.
- Nuttli, O.W., Average seismic source-parameter relations for mid-plate earthquakes, *Bull. Seis. Soc. Am.*, 73, 519-535, 1983.

- Oppenheim, A.V. and R.W. Schaffer, Digital Signal Processing, Prentice-Hall, New Jersey, 585pp, 1975.
- Paul, A., D. Jongmans, M. Campillo, P. Malin, and D. Baumont, Amplitudes of regional seismic phases in relation to crustal structure of the Sierra Nevada, California, *J. Geophys. Res.*, 101, 25,243-25,254, 1996.
- Phillips, W.S., Empirical path corrections in Central China, submitted to *Geophys. Res. Lett.*, xxpp, 1997.
- Pomeroy, P.W., W.J. Best, and T.V. McEvelly, Test ban treaty verification with regional data-a review, *Bull. Seism. Soc. Am.*, 72, S89-S129, 1982.
- Rodgers, A.J., T. Lay, W.R. Walter, and K.M. Mayeda, Comparison of regional phase amplitude ratio measurement techniques, Lawrence Livermore National Laboratory, Livermore, CA, UCRL-JC-127080, submitted to *Bull. Seis. Soc. Am.*, 13pp, 1997.
- Sereno, T.J., S.R. Bratt, and T.C. Bache, Simultaneous inversion of regional wave spectra for attenuation and seismic moment in Scandinavia, *J. Geophys. Res.*, 93, 2019-2035, 1988.
- Taylor S.R., M.D. Denny, E.S. Vergino, and R.E. Glaser, Regional discrimination between NTS explosions and western U.S. earthquakes, *Bull. Seism. Soc. Am.*, 79, 1142-1176, 1989.
- Taylor, S.R. and M.D. Denny, An analysis of spectral differences between NTS and Shagan River nuclear explosions, *J. Geophys. Res.*, 96, 6237-6245, 1991.
- Taylor, S.R., Analysis of high-frequency Pg/Lg ratios from NTS explosions and western U.S. earthquakes, *Bull. Seism. Soc. Am.*, 86, 1042-1053, 1996.
- Taylor, S.R., and H.E. Hartse, An evaluation of generalized likelihood ratio outlier detection to identification of seismic events in western China, submitted to *Bull. Seis. Soc. Am.*, 15pp, 1997.
- Walter, W.R., K.M. Myeda, and H.J. Patton, Phase and spectral ratio discrimination between NTS earthquakes and explosions Part 1: Empirical observations, *Bull. Seism. Soc. Am.*, 85, 1050-1067, 1995.
- Zhang, T., S.Y. Schwartz, and T. Lay, Multivariate analysis of waveguide effects on short-period regional wave propagation in Eurasia and its application in seismic discrimination, *J. Geophys. Res.*, 99, 21,929-21,945, 1994.



MS Equation 2.0